Journal of Engineering Mathematics **37:** 289–303, 2000.

Temperature distribution in an array of moving cracks acting as heat sinks

THOMAS BOECK[1] and UTE BAHR[2]
[1]*Center for Physical Fluid Dynamics, Dept. of Mechanical Engineering, Dresden University of Technology, 01062 Dresden, Germany; e-mail: boeck@tfd.mw.tu-dresden.de*
[2]*Institute for Theoretical Physics, Dept. of Physics, Dresden University of Technology, 01062 Dresden, Germany*

Received 29 April 1998; accepted in revised form 10 February 1999

Abstract. The temperature distribution in a periodic array of parallel cracks acting as heat sinks is studied for the case of stationary crack motion by use of the Wiener–Hopf method. The problem arises in the investigation of cracks propagating into solid material, where the stresses driving crack motion are caused by heat transfer from the solid through the crack surfaces. The solution is given in terms of Fourier integrals involving infinite products. The heat-flux distribution in the vicinity of the crack tips is computed analytically from the high wavenumber asymptotics. Numerical solutions of the temperature distribution are presented for several values of the Biot and Péclet number, and the effect of varying these parameters is discussed qualitatively.

Key words: stationary crack propagation, heat diffusion, strip geometry, Wiener–Hopf technique.

1. Introduction

The fracturing of solid materials under external tension or shear is usually caused by dynamic propagation of cracks. Provided the external forces have supplied sufficient elastic energy, the cracks can traverse the entire body with velocities of the order of the speed of sound, leading to sudden, uncontrolled failure of the material [1, 2]. Controlled crack propagation can be achieved when the stresses driving crack motion are applied only in the vicinity of the crack tip. If the zone of increased tensile or shear stresses is moved with constant velocity v through the elastic body, then the resulting crack motion will attain the same velocity. In the modeling of this phenomenon, no dynamic processes need to be taken into account. Only the condition for static equilibrium of the crack has to be used. Yuse and Sano have realized such a controlled crack motion by lowering a strip of heated glass into cold water [3]. The cooling generates temperature gradients which give rise to thermal stresses in the vicinity of the crack tip. Depending on the applied temperature difference and lowering velocity v they observed various regimes of crack motion, *i.e.* straight and oscillatory motion of single or multiple cracks. Subsequent theoretical investigations have reproduced the bifurcation from straight to oscillatory motion as well as other aspects [4–7].

In a first approximation, the presence of cracks does not affect the heat transfer and the temperature distribution in the glass strip experiment. However, there may also be cases where the crack surfaces contribute significantly to the heat transfer. The temperature distribution then depends on the position of the cracks. This mechanism is important in the chemical decomposition of solids, which can be studied in the framework of linear thermoelasticity when the temperature field is replaced by a concentration field. The model proposed by Yakobson

[8] considers the decay of a compound into a gaseous and a solid component, which occupies a smaller volume fraction. The gaseous component diffuses through the material towards the surface, where it is removed from the solid. In [8], it is assumed that the decomposition gives rise to a moving front between the solid and the fragments. The concentration profile of the gaseous component in the solid is assumed one-dimensional. It allows for precursor cracks which move with the same velocity as the front. In contrast to the experiment of Yuse and Sano, the velocity of the crack front is not prescribed. Yakobson uses a stability argument as selection criterion for the velocity v.

The assumption of a front between solid and fragments is unnecessary when the surfaces of the precursor cracks are taken into account for removal of the gaseous component. If we ignore the fragmentation process, the cracks grow indefinitely, and cannot be considered separately. The simplest configuration one can consider in this case consists of a periodic array of evenly spaced cracks propagating with constant velocity. This problem has been analyzed by the authors using finite element computations for the case of internal cooling of the crack surfaces [9]. Since the analysis is based on linear thermoelasticity, it is mathematically equivalent to that of chemical decomposition when the latter is modelled as in [8].

Owing to its simple geometry, the Wiener–Hopf technique [10–12] is applicable for the solution of this problem. The solution is obtained in two steps. The temperature distribution must be computed first, since it occurs in the thermoelastic stress–strain relation. After that, the mechanical quantities, *i.e*. displacements and stresses, can be determined. Both the thermal and the mechanical problem can, in principle, be solved by the Wiener–Hopf method. The solution of the second step is an extension of the work by Benthem and Koiter [13], which treats a periodic array of cracks with constant tension on the crack surfaces. However, the mechanical problem leads to complex algebra and apparently requires extensive numerical computations.

In this paper, we derive the Wiener–Hopf solution for the temperature distribution in an array of cracks propagating with constant velocity. The Wiener–Hopf solution assures us of the existence of a solution with the desired asymptotics for the temperature distribution far away from the crack tips. Mathematically, it furnishes an example of a homogeneous Wiener–Hopf problem with a non-trivial solution.

The paper is organized as follows. We introduce the non-dimensional equations and parameters, and derive the Wiener–Hopf equation in Fourier space using Jones's method [10, pp. 52–58] in the following section. An infinite product representation of the solution is given in the third section. After that, we derive approximations for the heat flux in the vicinity of the crack tip and present numerically computed temperature distributions for several values of the non-dimensional parameters. Finally, we summarize our findings and indicate possible extensions of this work.

2. Formulation of the problem

We consider the temperature field in a periodic array of moving cracks filled with a coolant of temperature T_1. The cracks propagate with constant velocity v into a material of temperature $T = T_0$. We assume that the cracks are evenly spaced and parallel, *i.e*. their arrangement is similar to the teeth of a comb. The distance between the cracks is $2d$. We assume that the temperature is independent of the vertical z-direction. Because of symmetry we only need

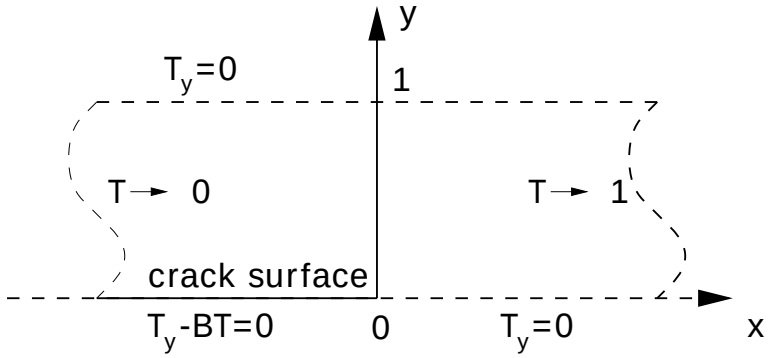

Figure 1. Schematic diagram of coordinate system and boundary conditions. The heat flux component T_y vanishes on the symmetry lines.

to consider a single crack. We choose the coordinate axes so that the crack moves along the x-axis. The symmetry domain extends from $y = 0$ to $y = d$.

For non-dimensionalization of the problem we choose d as unit of length, κ/d as unit of velocity, d^2/κ as unit of time, and $T_0 - T_1$ as unit of temperature. The origin of the dimensionless temperature scale corresponds to T_1. The quantity κ denotes the thermal diffusivity of the material. In the frame of reference moving with the cracks, the stationary heat equation for the temperature T reads

$$\nabla^2 T(x, y) + P\partial_x T(x, y) = 0, \quad P = \frac{vd}{\kappa}, \tag{1}$$

where the dimensionless velocity P is called the Péclet number. The boundary conditions are summarized in Figure 1. The heat flux across the crack surface $x < 0, y = 0$ is given by Newton's law of cooling,

$$\partial_y T = B\,T, \quad B = \frac{hd}{\lambda_c}, \tag{2}$$

where B is called the Biot number. The parameters entering the definition of B are the heat-transfer coefficient h between the solid material and the coolant inside the crack and the heat conductivity λ_c of the solid. Symmetry requires that no heat flux occurs on $x > 0$, $y = 0$ and on the line $y = 1$. The asymptotic behavior of T is such that $T \to 0$ as $x \to -\infty$ and $T \to 1$ as $x \to \infty$. In summary, the problem reads

$$\nabla^2 T(x, y) + P\partial_x T(x, y) = 0, \quad -\infty < x < \infty, \;\; 0 < y < 1, \tag{3}$$

$$\partial_y T = B\,T, \quad -\infty < x < 0, \;\; y = 0, \tag{4}$$

$$\partial_y T = 0, \quad 0 < x < \infty, \;\; y = 0, \quad \text{and} \quad -\infty < x < \infty, \;\; y = 1, \tag{5}$$

$$\lim_{x\to-\infty} T(x, y) = 0, \qquad \lim_{x\to+\infty} T(x, y) = 1, \quad 0 \leqslant y \leqslant 1. \tag{6}$$

For the solution, the Fourier transform $t(k, y)$ of $T(x, y)$ is needed. We use the definitions

$$t(k, y) = \frac{1}{2\pi}\int_{-\infty}^{\infty} \exp(-\mathrm{i}kx)T(x, y)\,\mathrm{d}x, \tag{7}$$

$$T(x, y) = \int_{-\infty-\mathrm{i}\varepsilon}^{\infty-\mathrm{i}\varepsilon} \exp(\mathrm{i}kx)t(k, y)\,\mathrm{d}k. \tag{8}$$

Convergence of (7) requires that the imaginary part $\Im\mathrm{m}(k)$ of the complex variable k is less than zero. Accordingly, the integration contour for the inverse transform (8) must be located below the real axis for convergence, which is indicated by the purely imaginary offset $-\mathrm{i}\varepsilon$ in the integration limits. In the following, we shall still write $-\infty$ and ∞ as integration limits also in such cases, but we will remark on the appropriate integration contour. Note that we use capital letters for the function in real space and small letters for its Fourier transform.

Upon inserting expression (8) into (1) we obtain

$$\left(\frac{\mathrm{d}^2}{\mathrm{d}y^2} - k^2 + \mathrm{i}kP\right) t(k, y) = 0. \tag{9}$$

The solution of this linear, second order, constant coefficient ordinary differential equation is of the form $t = \exp(\lambda y)$ with the characteristic equation

$$\lambda^2 - k^2 + \mathrm{i}kP = 0. \tag{10}$$

The roots are $\pm\lambda$ with

$$\lambda = \sqrt{k^2 - \mathrm{i}kP}, \tag{11}$$

where the square root maps positive reals to positive reals. The branch cut is made along the upper imaginary axis from 0 to $\mathrm{i}P$. The solution $t(k, y)$ takes the form

$$t(k, y) = A(k)\exp(\lambda y) + Z(k)\exp(-\lambda y). \tag{12}$$

The boundary condition on T at $y = 1$ requires that $(\partial t(k, y)/\partial y)|_{y=1} = 0$, hence

$$t(k, y) = 2A(k)\exp(\lambda)\cosh(\lambda(1 - y)). \tag{13}$$

We are now in a position to formulate the Wiener–Hopf equation. To this end we define two functions $U(x)$ and $V(x)$, which are derived from the boundary conditions on the crack line. They are given by

$$U(x) = T(x, 0) - \frac{1}{B}\partial_y T(x, y)|_{y=0}, \tag{14}$$

$$V(x) = \partial_y T(x, y)|_{y=0}. \tag{15}$$

The function $U(x)$ is zero for $x < 0$, and $V(x)$ is zero for $x > 0$. The Fourier transforms of these functions read

$$u(k) = t(k, 0) - \frac{1}{B}\partial_y t(k, y)|_{y=0}, \tag{16}$$

$$v(k) = \partial_y t(k, y)|_{y=0}. \tag{17}$$

Inserting (13) on the right-hand sides in the above equations and eliminating $A(k)$, we have

$$u(k) = f(k)v(k), \tag{18}$$

$$f(k) = -\frac{\cosh(\lambda) + \lambda\sinh(\lambda)/B}{\lambda\sinh(\lambda)}. \tag{19}$$

Equation (18) is the Wiener–Hopf equation with the kernel $f(k)$. We seek a non-trivial solution of this homogeneous equation, which gives the correct asymptotic behavior of the temperature.

3. Solution of the Wiener–Hopf equation

Because of the properties of the Fourier transform, u and v are analytic in those parts of the complex plane where their defining Fourier integrals converge [10, p. 23]. Assuming that $T(x, y = 0)$ and $\partial_y T(x, y = 0)$ are bounded functions of x, the integral for $u(k)$ will converge for $\mathfrak{Im}(k) < 0$. It is also reasonable to expect that $\partial_y T(x, y = 0)$ decays exponentially to zero as $x \to -\infty$, *i.e.* we may substitute an expression $\exp(\beta x)$ ($\beta > 0$) for $\partial_y T(x, y = 0)$ in the equation for $v(k)$. The Fourier integral for $v(k)$ will then converge for $\mathfrak{Im}(k) > -\beta$. The functions u and v should both be analytic in a strip $-\beta < \mathfrak{Im}(k) < 0$, where $\beta > 0$ is so far unknown. If a decomposition of $f(k)$ in the form $f(k) = f_+(k) f_-(k)$ can be found, where $f_+(k)$ is analytic and nonzero for $\mathfrak{Im}(k) > -\beta$ and $f_-(k)$ is analytic and nonzero for $\mathfrak{Im}(k) < 0$, we may write

$$\frac{u(k)}{f_-(k)} = q(k) = v(k) f_+(k). \tag{20}$$

The left-hand side and right-hand side in (20) are identical and analytic on the strip $-\beta < \mathfrak{Im}(k) < 0$. Therefore, they represent an uniquely defined analytic function $q(k)$. The function $q(k)$ is entire, since the left hand side of (20) represents q for $\mathfrak{Im}(k) > -\beta$ and the right-hand side represents q for $\mathfrak{Im}(k) < 0$. It has to be chosen such that the desired behavior of $u(k)$ and $v(k)$ is obtained.

The crucial step in the solution consists in decomposing the Wiener–Hopf kernel $f(k)$. It can be accomplished by inspection when infinite-product representations of the numerator and denominator are known. We shall derive these representations as follows. First, we write down the product representations with λ as independent variable. In the second step, λ is replaced by its actual representation as function of k.

Infinite-product representations of numerator and denominator are given by the infinite product theorem [10, p. 40]. The individual factors of the product contain the roots of $\cosh(\lambda) + \lambda \sinh(\lambda)/B$ and $\lambda \sinh(\lambda)$, respectively. We note that these roots are purely imaginary. Moreover, if λ is a root, its complex conjugate $\lambda^* = -\lambda$ will also be a root. For the numerator, all roots are simple. We denote by $\lambda_n = \mathrm{i} y_n$ the roots of $\cosh(\lambda) + \lambda \sinh(\lambda)/B$ with the imaginary part y_n in the interval $((n-1)\pi, (n-\frac{1}{2})\pi)$, where $n = 1, 2, \ldots$ runs through the positive integers.

Using the infinite product theorem, we have

$$\cosh(\lambda) + \lambda \sinh(\lambda)/B = \prod_{n=1}^{\infty} \left(\frac{y_n^2 + \lambda^2}{y_n^2} \right). \tag{21}$$

For the denominator, there are simple roots at $\pm \mathrm{i} n\pi$ (n positive integer) and a double zero at $\lambda = 0$. It follows that

$$\lambda \sinh(\lambda) = \lambda^2 \prod_{n=1}^{\infty} \left(\frac{n^2\pi^2 + \lambda^2}{n^2\pi^2} \right). \tag{22}$$

We shall now replace λ^2 by $k(k - \mathrm{i}P)$ in both Equation (21) and (22). The numerator $n^2\pi^2 + k^2 - \mathrm{i}kP$ can be written in the form $(k - k_n^{(1)})(k - k_n^{(2)})$, where $k_n^{(1)}$ and $k_n^{(2)}$ are the solutions of

$$n^2\pi^2 + k^2 - \mathrm{i}kP = 0. \tag{23}$$

The same applies for $y_n^2 + k^2 - \mathrm{i}kP$. Here we write

$$(k - \tilde{k}_n^{(1)})(k - \tilde{k}_n^{(2)}) = y_n^2 + k^2 - \mathrm{i}kP, \tag{24}$$

where $\tilde{k}_n^{(1/2)}$ are the roots of $y_n^2 + k^2 - \mathrm{i}kP = 0$. The explicit expressions are

$$k_n^{(1/2)} = \frac{\mathrm{i}P}{2} \pm \mathrm{i}\sqrt{\frac{P^2}{4} + n^2\pi^2}, \qquad \tilde{k}_n^{(1/2)} = \frac{\mathrm{i}P}{2} \pm \mathrm{i}\sqrt{\frac{P^2}{4} + y_n^2}. \tag{25}$$

We further note that $k_n^{(1)}k_n^{(2)} = n^2\pi^2$ and $\tilde{k}_n^{(1)}\tilde{k}_n^{(2)} = y_n^2$. With these definitions, the Equations (21) and (22) take the form

$$\lambda(k)\sinh(\lambda(k)) = k(k - \mathrm{i}P)\prod_{n=1}^{\infty}\left[\left(1 - \frac{k}{k_n^{(1)}}\right)\left(1 - \frac{k}{k_n^{(2)}}\right)\right], \tag{26}$$

$$\cosh(\lambda(k)) + \lambda(k)\sinh(\lambda(k))/B = \prod_{n=1}^{\infty}\left[\left(1 - \frac{k}{\tilde{k}_n^{(1)}}\right)\left(1 - \frac{k}{\tilde{k}_n^{(2)}}\right)\right]. \tag{27}$$

Notice that all of the roots $k_n^{(1)}$ and $\tilde{k}_n^{(1)}$ lie in the upper complex plane, *i.e.* their imaginary part is positive. Similarly, all of the roots $k_n^{(2)}$ and $\tilde{k}_n^{(2)}$ lie in the lower half plane. Based on this observation we decompose f as follows

$$f_-(k) = -\frac{1}{k(k - \mathrm{i}P)}\prod_{n=1}^{\infty}\frac{1 - k/\tilde{k}_n^{(1)}}{1 - k/k_n^{(1)}}, \tag{28}$$

$$f_+(k) = \prod_{n=1}^{\infty}\frac{1 - k/\tilde{k}_n^{(2)}}{1 - k/k_n^{(2)}}. \tag{29}$$

The function $f_-(k)$ is nonzero and analytic for $\Im\mathfrak{m}(k) < 0$, and $f_+(k)$ is nonzero and analytic for $\Im\mathfrak{m}(k) > -\beta$, where β is given by the modulus of the imaginary part of $\tilde{k}_1^{(2)}$.

The unknown function $u(k)$ is determined by $u(k) = q(k)f_-(k)$. The function $q(k)$ must be equal to a constant in order to satisfy the boundary conditions. This can be seen from the asymptotic expressions (A15, A17) for f_- as $|k| \to \infty$ given in the Appendix. The introduction of higher terms in the Taylor expansion of $q(k)$ would cause an asymptotic behavior of u incompatible with a bounded temperature. We will demonstrate this implicitly in the next section, where the heat flux in the vicinity of the crack tip and of the temperature profile along $y = 0$ are computed.

The value of the constant q can be obtained by considering the limit $k \to 0$. The function $U(x)$ is bounded and satisfies $U \to 1$ as $x \to \infty$. It is zero for $x < 0$. We denote by $\Theta(x)$ the step function taking the values 0 and 1 for $x < 0$ and $x \geqslant 0$, respectively. The function $U - \Theta$

is then integrable on the entire real axis, and the Fourier transform of $U - \Theta$ is a continuous function of the real variable k. The singularity of $u(k)$ at $k = 0$ thus coincides with that of the Fourier transform of $\Theta(x)$, which is $-\mathrm{i}/2\pi k$. Using (28), we find that

$$q = \lim_{k\to 0} \frac{u(k)}{f_-(k)} = \frac{-\mathrm{i}/2\pi k}{-\mathrm{i}/kP} = P/2\pi. \tag{30}$$

In summary, the functions $u(k)$ and $v(k)$ are given by

$$u(k) = Pf_-(k)/2\pi, \qquad v(k) = P/2\pi f_+(k). \tag{31}$$

The Fourier transform of the temperature reads

$$t(k, y) = t(k, 0)\frac{\cosh[(1-y)\lambda(k)]}{\cosh(\lambda(k))}, \tag{32}$$

$$t(k, 0) = u(k) + v(k)/B. \tag{33}$$

4. Temperature and heat-flux distribution

In this section we shall determine the behavior of the heat flux about the crack tip as well as the global temperature distribution. This will justify the choice of the constant function $q = P/2\pi$ used in the Wiener–Hopf procedure and clarify the nature of the crack tip singularity. To this end we need to know the asymptotic behavior of the functions f_+ and f_- as $|k| \to \infty$, which is derived in the Appendix.

4.1. Heat flux near the crack tip

The dimensionless heat flux $\partial_y T(x, y)$ in y-direction is given by the Fourier integral

$$\partial_y T(x, y) = \int_{-\infty}^{\infty} \exp(\mathrm{i}kx)\partial_y t(k, y)\,\mathrm{d}k, \tag{34}$$

where

$$\partial_y t(k, y) = -\frac{P}{2\pi}\frac{1}{f_+(k)}\frac{\mathrm{e}^{-\lambda(1-y)} - \mathrm{e}^{\lambda(1-y)}}{\mathrm{e}^{\lambda} - \mathrm{e}^{-\lambda}} \tag{35}$$

for $y \geqslant 0$. We wish to determine the singular behavior of $\partial_y T$ near the crack tip. To this end we write

$$\begin{aligned}\partial_y T(x, y) \;=\; & \int_{-\infty}^{-K} \mathrm{e}^{\mathrm{i}kx}\partial_y t(k, y)\,\mathrm{d}k \\ & + \int_{-K}^{K} \mathrm{e}^{\mathrm{i}kx}\partial_y t(k, y)\,\mathrm{d}k + \int_{K}^{\infty} \mathrm{e}^{\mathrm{i}kx}\partial_y t(k, y)\,\mathrm{d}k,\end{aligned} \tag{36}$$

and assume that $K > 0$ is sufficiently large so that we can substitute asymptotic approximations for the integrands $\partial_y t(k, y)$ in the first and third term of the right-hand side. These approximations are valid in the limit $k \to -\infty$ and $k \to +\infty$, respectively. The second integral in (36) clearly gives a continuous function of x because $\partial_y t(k, y)$ is a bounded function of k and will therefore be ignored.

For $0 \leqslant y \leqslant 1$ we have the asymptotic relation

$$\frac{\mathrm{e}^{-\lambda(1-y)} - \mathrm{e}^{\lambda(1-y)}}{\mathrm{e}^{\lambda} - \mathrm{e}^{-\lambda}} \sim -\mathrm{e}^{-|k|y} \tag{37}$$

for $k \to \pm\infty$. The relations (A20, A21) for $f_+(k)$ as $k \to \pm\infty$ are given at the end of the Appendix. Multiplying these expressions with the right-hand side of (37), we obtain the asymptotic expressions for $\partial_y t(k, y)$ to be used in Equation (36). We consider infinite Biot number first. Equation (36) then becomes

$$\partial_y T(x, y) \sim \frac{P}{2E\pi\sqrt{\pi}} \left(\int_{-\infty}^{-K} \frac{\mathrm{e}^{\mathrm{i}kx+ky-\mathrm{i}\pi/4}}{\sqrt{-k}}\,\mathrm{d}k + \int_{K}^{\infty} \frac{\mathrm{e}^{\mathrm{i}kx-ky+\mathrm{i}\pi/4}}{\sqrt{k}}\,\mathrm{d}k \right). \tag{38}$$

We can take the limit $K \to 0$ in (38) because this only results in an additional finite contribution for any x, y and thus does not modify the singular behavior.

Using the relation

$$\int_0^{\infty} \frac{\mathrm{e}^{-ax}}{\sqrt{x}}\mathrm{d}x = \sqrt{\frac{\pi}{a}}, \quad \mathfrak{Re}(a) > 0, \tag{39}$$

we then find

$$\partial_y T(x, y) \sim \frac{P}{\pi E} \frac{1}{\sqrt{r}} \sin(\varphi/2), \tag{40}$$

where $x + \mathrm{i}y = r\exp(\mathrm{i}\varphi)$. The constant E is defined in Equation (A10) in the Appendix. The asymptotic expression for the dimensionless heat flux on the crack is

$$\partial_y T(x, 0)|_{x<0} \sim \frac{P}{\pi E\sqrt{-x}}. \tag{41}$$

For finite B we again replace the integrands in Equation (36) by their asymptotic approximations, but we now use (A21) instead of (A20). We find

$$\partial_y T(x, y) \sim -\frac{PB}{2\pi^2 E} \left(\int_{-\infty}^{-K} \frac{\mathrm{e}^{\mathrm{i}kx+ky}}{\mathrm{i}k}\,\mathrm{d}k + \int_{K}^{\infty} \frac{\mathrm{e}^{\mathrm{i}kx-ky}}{\mathrm{i}k}\,\mathrm{d}k \right), \tag{42}$$

where E is now defined by Equation (A12). The additional contribution incurred by taking the limit $K \to 0$ in (42) reads

$$-\frac{PB}{2\pi^2 E} \left(\int_0^{K} \frac{2\sin(kx)}{k}\,\mathrm{e}^{-ky}\mathrm{d}k \right), \tag{43}$$

which becomes zero as $x \to 0$. It will therefore not modify the singularity at the crack tip. We then differentiate the right hand side of (42) with respect to the variable y and take $K \to 0$. Evaluation of the resulting expressions is straightforward, giving

$$\partial_{yy} T(x, y) \sim \frac{PB}{\pi^2 E} \frac{x}{x^2 + y^2}. \tag{44}$$

The integration with respect to y can be performed analytically. We obtain

$$\partial_y T(x, y) \sim \frac{PB}{\pi E} \frac{\varphi}{\pi} \tag{45}$$

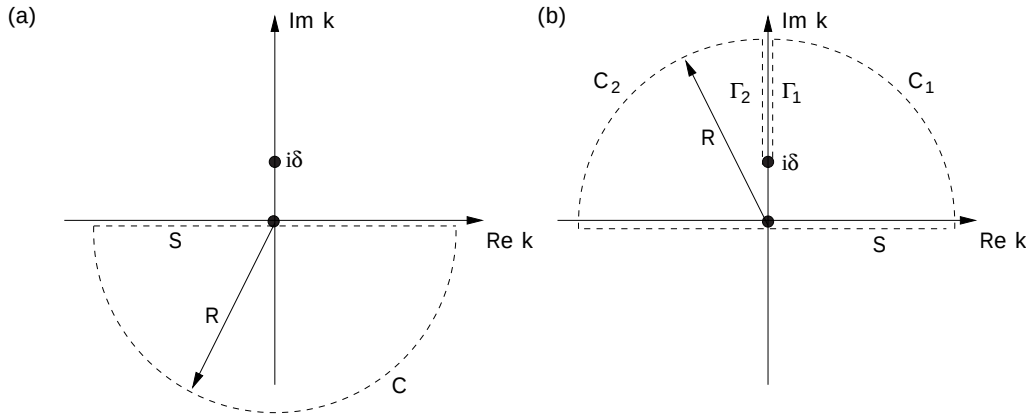

Figure 2. Integration contours for the Fourier transform of $W(x)$ for $x < 0$ (a) and $x > 0$ (b) for the case of infinite Biot number.

up to a function of x only. This function must be zero since $\partial_y T(x, y)\big|_{y=0} = 0$ for positive x. The heat flux on the crack line near the crack tip reads

$$\partial_y T(x, 0)|_{x<0} \sim \frac{PB}{\pi E}. \tag{46}$$

4.2. Temperature distribution

The numerical computation of the temperature distribution can be divided into two separate steps. First, we compute the temperature distribution $T(x, 0)$ on the crack line. When this function is known, the temperature in the entire domain can be obtained from a convolution integral involving $T(x, 0)$ and a kernel depending only on x, y and the Péclet number P, *cf.* Equation (32, 33).

The temperature $T(x, 0)$ can be expressed in terms of $U(x)$ and $V(x)$ as

$$T(x, 0) = U(x) + V(x)/B. \tag{47}$$

It simplifies to $T(x, 0) = U(x)$ for $B \to \infty$. The functions $U(x)$ and $V(x)$ must be obtained from their Fourier transforms $u(k)$ and $v(k)$. The numerical evaluation of the Fourier transforms requires a cutoff in the evaluation of the infinite products representing u and v as well as a cutoff in the range for the contour integration. The divergent parts cannot be treated numerically. We subtract certain approximations off of $u(k)$ and $v(k)$ so that the remainders are decaying faster than $1/k$ at infinity and are bounded at $k = 0$. This approach ensures that the truncated infinite product is sufficiently converged because it has to reproduce the proper asymptotics also for large $|k|$.

In the case of infinite Biot number the following function $w(k)$ approximates $u(k)$ near $k = 0$ as well as for $|k| \to \infty$

$$w(k) = -\frac{P\,\mathrm{e}^{\mathrm{i}\pi/4}}{2\pi E k\sqrt{k - \mathrm{i}\delta}}, \quad \delta = (P/E)^2. \tag{48}$$

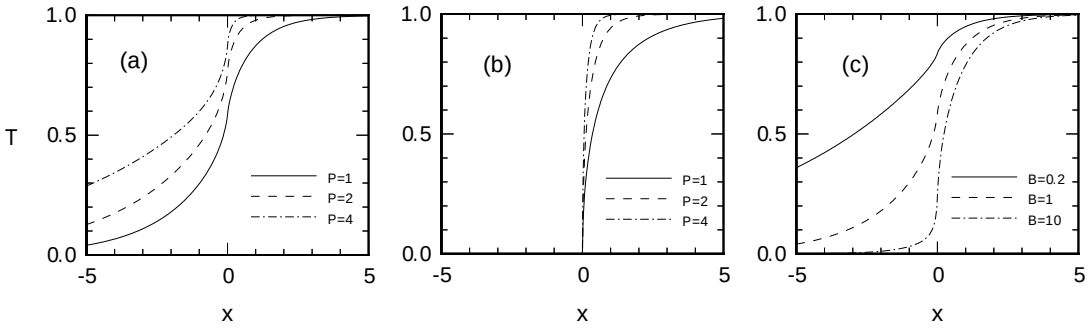

Figure 3. Temperature profiles along the crack line $y = 0$. Figures (a) ($B = 1$) and (b) (B infinite) show profiles for fixed Biot number and different Péclet numbers. In (c), the Péclet number is fixed to $P = 1$.

The Fourier transform

$$W(x) = \int_{-\infty}^{\infty} \exp(\mathrm{i}kx)w(k)\,\mathrm{d}k \tag{49}$$

can be evaluated using Jordan's lemma and the residue theorem. The integration path must lie in the strip, *i.e.* below the real axis, but arbitrarily close to it. For $x < 0$, we can close the integration contour by a semi-circle of radius $R \to \infty$ in the lower half plane, *cf.* Figure 2(a). The integral is zero by the residue theorem.

In the case $x > 0$, the semi-circle of radius $R \to \infty$ must reside in the upper half plane as shown in Figure 2(b). The circle does not cross the branch cut from $\mathrm{i}\delta$ to ∞. The contributions of the circular arcs C_1 and C_2 vanish as $R \to \infty$, but a contribution comes from the integration along the branch cut and from the residue at $k = 0$. We take $k - \mathrm{i}\delta = \xi \exp(\mathrm{i}\pi/2)$ on Γ_1 and $k - \mathrm{i}\delta = \xi \exp(-\mathrm{i}3\pi/2)$ on Γ_2 ($\xi \geqslant 0$). This gives $\sqrt{k - \mathrm{i}\delta} = \sqrt{\xi}\exp(\mathrm{i}\pi/4)$ on Γ_1 and $\sqrt{k - \mathrm{i}\delta} = \sqrt{\xi}\exp(-\mathrm{i}3\pi/4)$ on Γ_2. With these definitions, it follows that

$$\int_{\Gamma_1 \cup \Gamma_2} \exp(\mathrm{i}kx)w(k)\,\mathrm{d}k = \frac{P}{E\pi}\int_0^{\infty} \frac{\exp(-x\xi - x\delta)}{(\delta + \xi)\sqrt{\xi}}\,\mathrm{d}\xi. \tag{50}$$

This integral can be evaluated exactly using computer algebra software [15]. The final result for $W(x)$ reads

$$W(x) = \begin{cases} 0: & x < 0, \\ \operatorname{erf}(\sqrt{x\delta}): & x \geqslant 0. \end{cases} \tag{51}$$

Here $\operatorname{erf}(z)$ denotes the error function defined by

$$\operatorname{erf}(z) = \frac{2}{\sqrt{\pi}}\int_0^z \exp(-t^2)\,\mathrm{d}t. \tag{52}$$

In the case of finite Biot number we can take composite approximations

$$f_+ \sim 1 - \frac{E\pi\,\mathrm{i}k}{B}, \qquad f_- \sim \frac{1}{\mathrm{i}P}\left(\frac{1}{k} - \frac{1}{k + \mathrm{i}\varepsilon}\right) + \frac{1}{\mathrm{i}E\pi}\frac{1}{k + \mathrm{i}\varepsilon}, \tag{53}$$

which correctly reflect the behavior near $k = 0$ and for large $|k|$. The parameter ε is assumed to be an arbitrary positive number. The Fourier transforms of the corresponding approximations

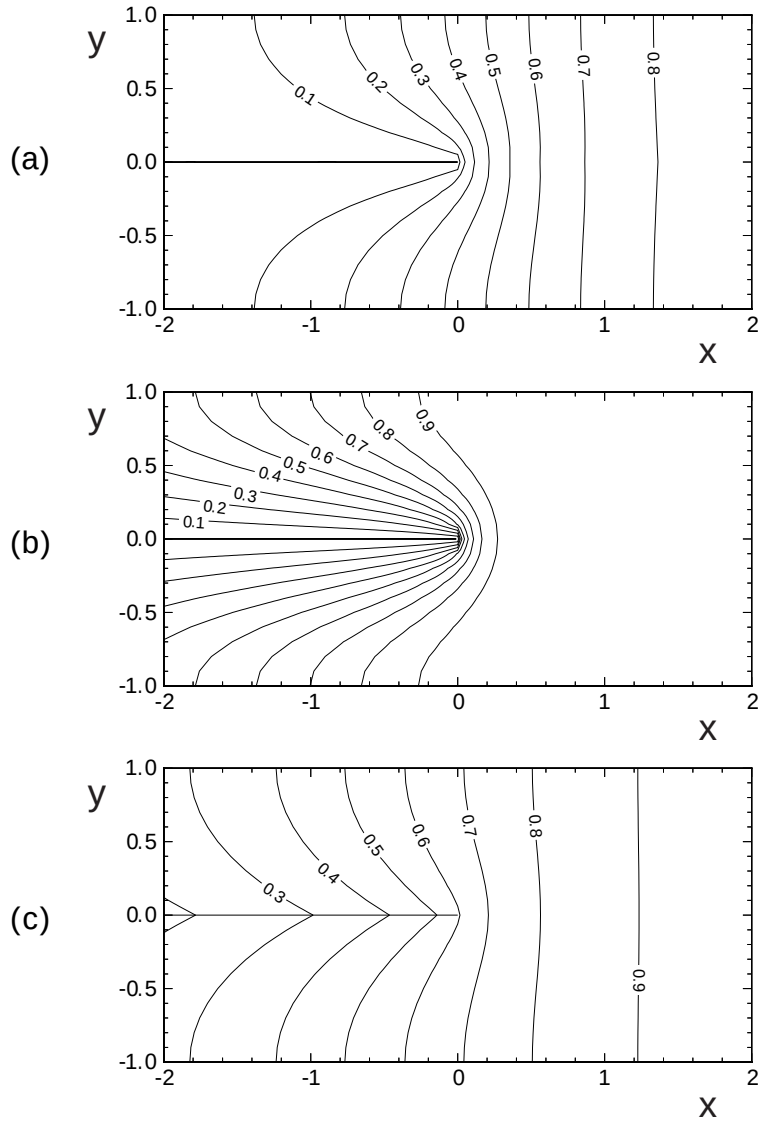

Figure 4. Isotherms for different sets of parameters. The Biot number is infinite in (a) and (b) with Péclet numbers $P = 1$ (a) and $P = 5$ (b); (c) shows the case $B = P = 1$.

to u and v are easily evaluated by Jordan's lemma and the residue theorem. The Fourier transforms of the remainders can be computed numerically.

Figures 3(a–c) show numerically computed temperature profiles on $y = 0$ for various values of P and B. The profile results from the interplay of two physical effects. Increasing P causes higher temperatures in between the cracks as more heat must be removed per unit time when the motion is faster. This causes higher temperatures near the crack tip and a slower decay along the crack since the heat flux is proportional to the temperature difference. The temperature profiles for $B = 1$ and different values of P of Figure 3(a) illustrate this effect. The slower decay along the crack is less pronounced when B increases, and it eventually disappears for infinite B. Figure 3(b) shows temperature profiles for this case. For fixed P,

increasing B leads to a higher heat flux and therefore to lower temperatures. In particular, the temperature drop in the vicinity of the crack tip becomes steeper since more heat can be transferred per unit area of the crack surface. This is obvious from Figure 3(c).

We have also computed the solution in the entire domain. Figures 4(a–c) show isotherms in the vicinity of the crack tip for finite and infinite B. For infinite B, the crack line itself corresponds to the zero isotherm. By contrast, for finite B, isotherms end in the crack line. The persistence of high temperatures in between the cracks for large values of P is obvious from Figure 4(b).

All computations reported in this section were performed using 10^4 terms in the truncated infinite products and a cutoff wavenumber of 50π. The numerical computation of the Fourier transforms was carried out using the discrete Fast Fourier transform [14, Chapter 12] with 4096 data points. The computations typically require less than five minutes on a Pentium class PC.

5. Summary and conclusions

We have computed the temperature distribution in a two-dimensional array of parallel cracks moving with constant velocity by the Wiener–Hopf method. The heat transfer from the initially isothermal material to the crack is modeled by Newton's law of cooling. The dimensionless parameters of the problem are the Péclet number P and the Biot number B. The former parameter measures the strength of convective heat transport. The Biot number B describes the ratio of the heat flux across the crack interface to the typical heat flux in the bulk.

The Wiener–Hopf integral equation is derived using Jones's method [10, pp. 52–58]. Although the equation is homogeneous, a non-trivial solution is obtained because of the inhomogeneous boundary conditions on the temperature at infinity. The factorization of the Wiener–Hopf kernel into two analytic functions can be performed by means of infinite product representations. We have determined the asymptotic behavior of the factors analytically as well as the heat flux distribution in the vicinity of the crack tip.

The computation of the full temperature distribution cannot be done analytically. The numerical solution can be divided into two steps. The first step comprises the computation of the temperature profile along the crack line. After that, the temperature distribution in the entire domain can be obtained from a convolution integral involving the crack line temperature profile.

In the limit of infinite Biot number the heat flux density at the crack tip diverges. This case corresponds to prescribed zero temperature on the crack surface. For finite Biot number, heat flux density experiences a finite jump when the crack tip is crossed along the crack line. Higher Péclet numbers allow for higher temperatures between the cracks since convection becomes more important. Higher Biot numbers increase the heat transfer across the crack surface, which reduces the temperature.

The next step in a complete treatment of the problem would consist in the solution of the mechanical problem for the stress and displacement fields. The Wiener–Hopf method is applicable in principle also to this problem, but it seems hardly possible to make progress without resorting to extensive numerical computations as it will require the factorization of expressions involving the temperature field, which is given only in terms of an infinite product. A purely numerical treatment of the full problem of the stationary motion of an array of

parallel cracks driven by thermal cooling has been undertaken by the authors using finite elements [9].

Appendix. Asymptotic behavior of $f_{\pm}(k)$ for large $|k|$

Here we determine the asymptotic behavior for $k \to \infty$ of

$$\prod_{n=1}^{\infty} \frac{1 - k/\tilde{k}_n}{1 - k/k_n} \quad \text{where} \quad \begin{matrix} k_n = an + b + O(1/n), \\ \tilde{k}_n = an + b + c + O(1/n), \end{matrix} \quad \text{as } n \to \infty. \tag{A1}$$

Of interest are eventually only the particular cases $c/a = -\frac{1}{2}$ and $c/a = -1$ corresponding to infinite and finite Biot number, respectively. In order to obtain convergent expressions for numerator and denominator in Equation (A1) we write

$$\prod_{n=1}^{\infty} \frac{1 - k/\tilde{k}_n}{1 - k/k_n} = \frac{\prod_{n=1}^{\infty}(1 - k/\tilde{k}_n)\mathrm{e}^{k/an}}{\prod_{n=1}^{\infty}(1 - k/k_n)\mathrm{e}^{k/an}}. \tag{A2}$$

We can now make use of the asymptotic representation

$$\prod_{n=1}^{\infty}(1 - k/\alpha_n)\mathrm{e}^{k/an} \sim \mathrm{e}^{\gamma k/a} \frac{\Gamma(\beta/a + 1)}{\Gamma(-k/a + \beta/a + 1)} \prod_{n=1}^{\infty} \frac{an + \beta}{\alpha_n}, \tag{A3}$$

given in [10, p. 128], where $\alpha_n = an + \beta + O(1/n)$, β arbitrary. The symbols $\Gamma(x)$ and γ denote the Gamma function and Euler's constant (0·5772 . . .). We then have

$$\prod_{n=1}^{\infty} \frac{1 - k/\tilde{k}_n}{1 - k/k_n} \sim \frac{\Gamma(b/a + c/a + 1)\Gamma(-k/a + b/a + 1)}{\Gamma(b/a + 1)\Gamma(-k/a + b/a + c/a + 1)} \times \prod_{n=1}^{\infty} \frac{an + b + c}{an + b} \frac{k_n}{\tilde{k}_n},$$

which may be simplified further using

$$\frac{\Gamma(a + b)}{\Gamma(a)} \sim a^b \quad \text{as } a \to \infty, \ \ |\arg a| < \pi, \tag{A4}$$

which is readily derived from Stirling's formula [16]. We find

$$\prod_{n=1}^{\infty} \frac{1 - k/\tilde{k}_n}{1 - k/k_n} \sim \frac{1}{E} \left(-\frac{k}{a}\right)^{-c/a}. \tag{A5}$$

The constant $1/E$ collects the factors which are independent of k

$$\frac{1}{E} = \frac{\Gamma(b/a + c/a + 1)}{\Gamma(b/a + 1)} \prod_{n=1}^{\infty} \frac{an + b + c}{an + b} \frac{k_n}{\tilde{k}_n}. \tag{A6}$$

We will now simplify E for the special cases of interest.

Case $c/a = -\frac{1}{2}$
Consider the following relation [10, p. 41]

$$\prod_{n=1}^{\infty} \left(1 - \frac{\alpha}{an + \beta}\right) \mathrm{e}^{\alpha/an} = \mathrm{e}^{\gamma\alpha/a} \frac{\Gamma(\beta/a + 1)}{\Gamma(-\alpha/a + \beta/a + 1)} \tag{A7}$$

for the two cases $\alpha = c,\ \beta = b + c$ and $\alpha = -c,\ \beta = 0$. Upon multiplication we find

$$\frac{\Gamma(b/a + c/a + 1)}{\Gamma(b/a + 1)} = \Gamma(c/a + 1) \prod_{n=1}^{\infty} \frac{(an + c)(an + b)}{an(an + b + c)}, \tag{A8}$$

where $\Gamma(1) = 1$ has been used. Inserting this result into Equation (A6) for $1/E$ and observing that $\Gamma(c/a + 1) = \Gamma(\frac{1}{2}) = \sqrt{\pi}$ we obtain

$$\frac{1}{E} = \sqrt{\pi} \prod_{n=1}^{\infty} \frac{n - \frac{1}{2}}{n} \frac{k_n}{\tilde{k}_n}. \tag{A9}$$

Case $c/a = -1$
We extract the first factor $(an+b-a)/(an+b)$ (with $n = 1$) from the product in Equation (A6) and use $\Gamma(x + 1) = x\Gamma(x)$. This gives

$$\frac{1}{E} = \frac{1}{1 + b/a} \prod_{n=2}^{\infty} \frac{an + b - a}{an + b} \frac{k_{n-1}}{\tilde{k}_{n-1}}. \tag{A10}$$

After replacing $n \to n + 1$ we write $1/E$ in the form

$$\frac{1}{E} = \frac{1}{1 + b/a} \prod_{n=1}^{\infty} \frac{n + b/a}{n + 1 + b/a} \frac{n + 1}{n} \prod_{n=1}^{\infty} \frac{n}{n + 1} \frac{k_n}{\tilde{k}_n}. \tag{A11}$$

The first infinite product is again expressible by Gamma functions. Using (A8) for $c = a$, we find

$$\frac{1}{E} = \prod_{n=1}^{\infty} \frac{n}{n + 1} \frac{k_n}{\tilde{k}_n}. \tag{A12}$$

Now we determine the asymptotic expressions for

$$f_-(k) = -\frac{1}{k(k - \mathrm{i}P)} \prod_{n=1}^{\infty} \frac{1 - k/\tilde{k}_n^{(1)}}{1 - k/k_n^{(1)}}. \tag{A13}$$

For infinite Biot number we have

$$\tilde{k}_n^{(1)} = \mathrm{i}(n\pi + P/2 - \pi/2) + O(1/n), \qquad k_n^{(1)} = \mathrm{i}(n\pi + P/2) + O(1/n). \tag{A14}$$

Thus $a = \mathrm{i}\pi$, $b = \mathrm{i}P/2$, $c = -\mathrm{i}\pi/2$, $c/a = -\frac{1}{2}$, and with (A5) it follows that

$$f_-(k) \sim \frac{1}{E\sqrt{\pi}} \left(\frac{1}{\mathrm{i}k}\right)^{3/2} \quad \text{where} \quad \frac{1}{E} = \sqrt{\pi} \prod_{n=1}^{\infty} \frac{n - \frac{1}{2}}{n} \frac{k_n^{(1)}}{\tilde{k}_n^{(1)}}. \tag{A15}$$

For finite Biot number we have

$$\tilde{k}_n^{(1)} = \mathrm{i}(n\pi + P/2 - \pi) + O(1/n), \qquad k_n^{(1)} = \mathrm{i}(n\pi + P/2) + O(1/n), \tag{A16}$$

thus $a = \mathrm{i}\pi$, $b = \mathrm{i}P/2$, $c = -\mathrm{i}\pi$, $c/a = -1$. This gives

$$f_-(k) \sim \frac{1}{E\pi} \frac{1}{\mathrm{i}k} \quad \text{where} \quad \frac{1}{E} = \prod_{n=1}^{\infty} \frac{n}{n + 1} \frac{k_n^{(1)}}{\tilde{k}_n^{(1)}}. \tag{A17}$$

For the asymptotic behavior of $f_+(k)$ we use the definition

$$f_-(k)\,f_+(k) = -\frac{\cosh\lambda + \lambda\sinh\lambda/B}{\lambda\sinh\lambda} \tag{A18}$$

and determine the asymptotic behavior of the kernel on the right-hand side. We must again distinguish finite and infinite B. For infinite B

$$f_+(k) \sim -\frac{1}{kf_-(k)} \sim -\mathrm{i}E\sqrt{\pi}\,\sqrt{\mathrm{i}k}. \tag{A19}$$

To get the right sign of the root for real values of k we observe that $f_+^*(-k) = f_+(k)$. This is a consequence of $\partial_y T(x, y)$ being a real function. We find

$$f_+(k) \sim \begin{cases} \sqrt{\pi}E\,\mathrm{e}^{-\mathrm{i}\pi/4}\sqrt{k}, & k \to +\infty, \\ \sqrt{\pi}E\,\mathrm{e}^{\mathrm{i}\pi/4}\sqrt{-k}, & k \to -\infty. \end{cases} \tag{A20}$$

For finite B the kernel on the right-hand side of (A18) approaches $1/B$, hence

$$f_+(k) \sim -\frac{\pi E}{B}\mathrm{i}k. \tag{A21}$$

References

1. M. Marder and J. Fineberg, How things break. *Physics Today* 49(9) (1996) 24–29.
2. L. B. Freund, *Dynamic Fracture Mechanics*. Cambridge: Cambridge University Press (1998) 581pp.
3. A. Yuse and M. Sano, Transition between crack patterns in quenched glass plates. *Nature* 362 (1993) 329–331.
4. M. Marder, Instability of a crack in a heated strip. *Phys. Rev. E* 49(1) (1994) R51–R54.
5. S. Sasa, K. Sekimoto and H. Nakanishi, Oscillatory instability of crack propagations in quasistatic fracture. *Phys. Rev. E* 50(3) (1994) R1733–R1736.
6. M. Adda-Bedia and Y. Pomeau, Crack instabilities of a heated glass strip. *Phys. Rev. E* 52(4) (1995) 4105–4113.
7. H.-A. Bahr, A. Gerbatsch, U. Bahr and H.-J. Weiß, Oscillatory instability in thermal cracking: a first order phase-transition phenomenon. *Phys. Rev. E* 52(1) (1995) 240–243.
8. B. I. Yakobson, Morphology and rate of fracture in chemical decomposition of solids. *Phys. Rev. Lett.* 67 (1991) 1590–1593.
9. T. Boeck, H.-A. Bahr, S. Lampenscherf and U. Bahr, Self-driven propagation of crack arrays: a stationary two-dimensional model. Editorially approved for publication in *Phys. Rev. E*.
10. B. Noble, *Methods Based on the Wiener–Hopf Technique for the Solution of Partial Differential Equations*. Oxford: Pergamon Press (1958) 256pp.
11. G. F. Carrier, M. Krook and C. E. Pearson, *Functions of a Complex Variable*. New York: McGraw-Hill (1966) 438pp.
12. D. G. Duffy, *Transform Methods for Solving Partial Differential Equations*. Boca Raton: CRC Press (1994) 512pp.
13. J. P. Benthem and W. T. Koiter, Asymptotic approximations to crack problems. In: G. C. Sih (ed.), *Mechanics of Fracture*, vol. 1. Leiden: Noordhoff International Publishing (1973) 131–178.
14. W. H. Press, B. P. Flannery, S. A. Teukolsky and W. T. Vetterling, *Numerical Recipes in FORTRAN*. Cambridge: Cambridge University Press (1993) 992pp.
15. Wolfram Research, Inc., *Mathematica*. Version 2.2. (1995).
16. M. Abramowitz and I. A. Stegun (eds.), *Handbook of Mathematical Functions*. Frankfurt: Harri Deutsch (1984) 468pp.